

# Pressure-Induced Sequential Orbital Reorientation in a Magnetic Framework Material\*\*

Gregory J. Halder,\* Karena W. Chapman, John A. Schlueter, and Jamie L. Manson

The molecular understanding, control and prediction of functional materials behavior is not only of immense fundamental significance, but also represents a crucial step toward important wide-ranging applications.<sup>[1]</sup> Towards this, magnetic coordination materials are appealing because of their structural versatility and the accessibility of their low-energy spin exchange interactions. In particular, materials based on Jahn–Teller (JT) active metal centers,<sup>[2]</sup> where their magnetic orbitals are oriented relative to an elongated JT axis, allow the magnetic properties to be rationally modified through perturbation of the coordination environment. Pressure provides a potent means for achieving such perturbations,<sup>[3]</sup> however, accomplishing this in a predictable manner has remained elusive and largely unexplored.

The Jahn–Teller (JT) effect is fundamental to coordination chemistry with far-reaching implications on structure and function behaviors spanning high- $T_c$  superconductivity and colossal magnetoresistance.<sup>[2]</sup> In a traditional  $ML_6$  system, where the JT-active center is coordinated to identical ligands, the elongation of neighboring centers is uncorrelated unless there are cooperative interactions (e.g., crystal packing influences). However, when the metal is coordinated to a mixture of ligands, the differing crystal field strengths of the ligands will preferentially stabilize one of the possible JT orientations.<sup>[4]</sup> In  $Cu^{II}$  JT systems, the magnetic orbital ( $d_{x^2-y^2}$ ) is oriented along the Cu–L bonds in the equatorial  $CuL_4$  plane, perpendicular to the elongated JT axis ( $z$ ). As such, their magnetic characteristics are implicitly dictated by the JT

orientation and may be manipulated by perturbing the ligand coordination environment.

Here we exploit the powerful influence of pressure on atomic structure to control the magnetic properties of a  $Cu^{II}$ -based coordination network,  $CuF_2(H_2O)_2(pyz)$  ( $pyz$  = pyrazine).<sup>[5]</sup> In this material,  $pyz$ -bridged linear  $Cu^{II}$  chains (Figure 1a) are linked perpendicularly by very strong  $OH\cdots F$  hydrogen bonds to form a quasi-three-dimensional network (Figure 1b). As prepared, the JT axis is oriented along the chain direction, with elongated N–Cu–N bonds, such that the magnetic orbital is directed along the Cu–L bonds of the  $CuO_2F_2$  plane. This underlies its magnetic properties where the two-dimensional antiferromagnetic lattice is propagated through the Cu–OH $\cdots$ F–Cu connections of the two-dimensional hydrogen-bond network.

The impact of pressure on the atomic structure of  $CuF_2(H_2O)_2(pyz)$  was probed within a diamond anvil cell using synchrotron-based powder diffraction methods. The diffraction data exhibit a series of abrupt structural transitions at 0.9 GPa and 3.1 GPa (Figure 2) that are reversible upon

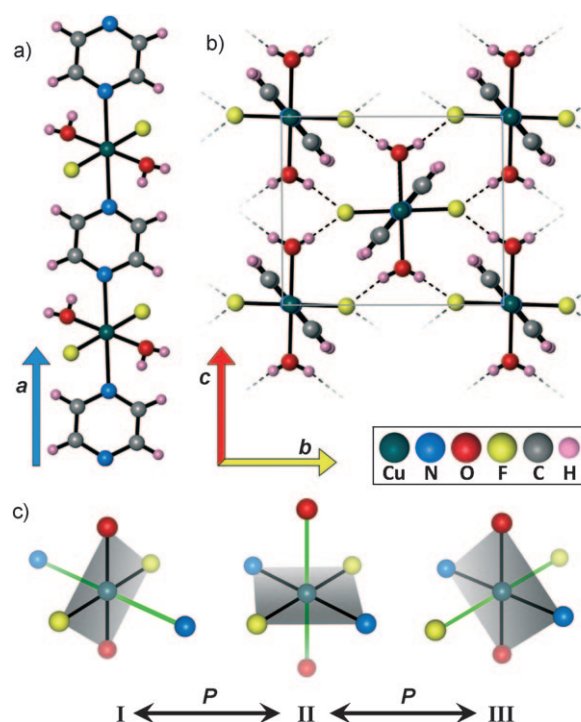


**Figure 1.** a) An isolated  $CuF_2(H_2O)_2(pyz)$  chain along the  $a$  direction, and b) the 2D hydrogen bonding network in the  $bc$  plane in the crystal structure of  $CuF_2(H_2O)_2(pyz)_2$ . c) The pressure-induced switching of the elongated JT-axis (green) of the  $CuF_2O_2N_2$  octahedra (gray planes contain the magnetic orbital).

[\*] Dr. G. J. Halder, Dr. J. A. Schlueter  
 Materials Science Division, Argonne National Laboratory  
 9700 South Cass Ave, Argonne, IL 60439 (USA)  
 E-mail: halder@aps.anl.gov

Dr. G. J. Halder, Dr. K. W. Chapman  
 X-ray Science Division, Argonne National Laboratory (USA)

Dr. J. L. Manson  
 Department of Chemistry & Biochemistry  
 Eastern Washington University (USA)

[\*\*] Work performed at Argonne National Laboratory and use of the Advanced Photon Source were supported by the U.S. Department of Energy, Office of Science, Office of Basic Energy Sciences, under Contract No. DE-AC02-06CH11357. Part of the pressure cell preparation used the GSECARS facility (Sector 13), Advanced Photon Source, Argonne National Laboratory. GSECARS is supported by the NSF-Earth Sciences (EAR-0622171) and DOE-Geosciences (DE-FG02-94ER14466). Work at EWU was partially supported by the National Science Foundation under Grant No. DMR-1005825.

Supporting information for this article is available on the WWW under <http://dx.doi.org/10.1002/anie.201003380>.

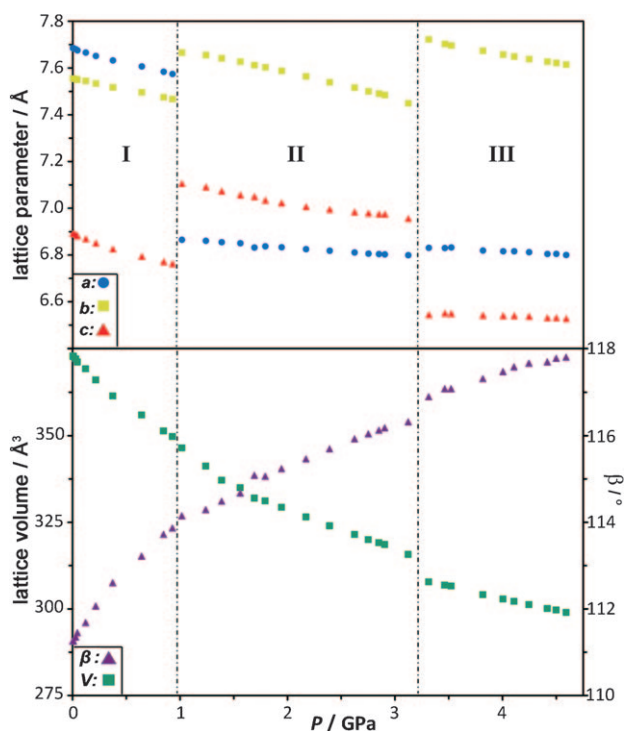


**Figure 2.** Pressure-induced changes in the lattice dimensions (*a*, *b*, and *c*), volume (*V*) and  $\beta$  angle for  $\text{CuF}_2(\text{H}_2\text{O})_2(\text{pyz})$ . Errors are within the size of the data points.

release of pressure. Despite pronounced discontinuities in the diffraction data, the structural symmetry remains unchanged (monoclinic,  $P2_1/c$ ). Instead, the abrupt transitions involve spontaneous changes in the *a*, *b*, and *c* lattice dimensions. The first transition (phase I  $\rightarrow$  phase II) at 0.9 GPa is characterized by a contraction of the *a*-axis with concomitant expansions of the *b*- and *c*-axes ( $\Delta a \approx -0.7 \text{ \AA}$ ,  $\Delta b \approx +0.2 \text{ \AA}$ ,  $\Delta c \approx +0.3 \text{ \AA}$ ). The second transition (phase II  $\rightarrow$  phase III) at 3.1 GPa is characterized by a contraction of the *c*-axis and an expansion of the *b*-axis ( $\Delta a \approx 0 \text{ \AA}$ ,  $\Delta b \approx +0.3 \text{ \AA}$ ,  $\Delta c \approx -0.4 \text{ \AA}$ ). The total lattice volume, and  $\beta$  angle of the monoclinic unit cell, vary approximately continuously through each transition (Figure 2) and correspond to a zero pressure bulk modulus ( $K_0$ ) of 12.1(6) GPa with  $K' = 4.6(4)$ . The discontinuities in the *a*-, *b*- and *c*-axes, along which the N–Cu–N, F–Cu–F and O–Cu–O bonds are principally oriented, reflect changes to these average bond lengths: for phase I,  $d_{\text{Cu-N}} \gg d_{\text{Cu-O}} \approx d_{\text{Cu-F}}$ ; for phase II  $d_{\text{Cu-O}} \gg d_{\text{Cu-N}} \approx d_{\text{Cu-F}}$ ; for phase III  $d_{\text{Cu-F}} \gg d_{\text{Cu-N}} \approx d_{\text{Cu-O}}$  (Supporting Information, Figure S6). As such, the observed transitions correspond to a reorientation of the JT-elongated axis from the N–Cu–N to the O–Cu–O to the F–Cu–F direction with increasing pressure (Figure 1c). Accordingly, the magnetic orbital re-orientates sequentially from the  $\text{CuF}_2\text{O}_2$  to the  $\text{CuF}_2\text{N}_2$  to the  $\text{CuN}_2\text{O}_2$  plane.

A single pressure-induced JT-switch has been observed in a handful of systems, including the  $\text{MO}_6$  octahedra in various Tutton salts  $[(\text{NH}_4)_2\text{M}(\text{H}_2\text{O})_6(\text{SO}_4)_2]$  for  $\text{M} = \text{Cr}, \text{Cu}$ <sup>[6,7]</sup> and the  $\text{MnF}_6$  octahedra in  $\text{Na}_3\text{MnF}_6$ .<sup>[8]</sup> In each of these cases only a single ligand-type surrounds the JT-active center, with the ligands subtly differentiated by pressure-dependent second-order intermolecular interactions. Here, the presence of

different ligands facilitates unprecedented sequential JT-switching that proceeds predictably in accordance with empirical ligand strengths (i.e., the spectrochemical series:  $\text{F}^- < \text{OH}_2 < \text{pyz}$ ).<sup>[9]</sup>

The general pressure-induced lattice compression reflects various different structural perturbations. The most significant contributions are associated with the “softer” components such as the  $\text{Cu}^{\text{II}}$  polyhedra and interchain interactions, whereas the fully conjugated pyz bridges are likely to be relatively rigid. While both bond angle distortions and bond compressions act to reduce the volume of the  $\text{Cu}^{\text{II}}$  polyhedra, due to the much lower energy of angular distortions these dominate the compression within the  $\text{Cu}^{\text{II}}$  octahedral.<sup>[10]</sup> This is reflected in the pressure dependence of the refined  $\text{Cu}^{\text{II}}$  coordination geometries, for which the most well defined trend is an increasing angular distortion of the  $\text{Cu}^{\text{II}}$  polyhedra with increasing pressure for each phase (Figure S7). Indeed, this is the dominant pressure-induced structural perturbation within the entire material. These angular distortions attain maxima at pressures immediately below the JT-switch, at which point the  $\text{Cu}^{\text{II}}$  geometry relaxes abruptly. The angular relaxation is possible—while still reducing  $\text{Cu}^{\text{II}}$  octahedral volume—because of the shorter average Cu–L bonds of successive JT isomers. These average Cu–L bond lengths are dictated by the JT-elongated bond lengths which decrease markedly with decreasing ligand field strength ( $d_{\text{Cu-N}} \gg d_{\text{Cu-O}} \gg d_{\text{Cu-F}}$ ), whereas the equatorial bond lengths remain relatively invariant. Presuming that the pressure-induced JT configurations are sequentially less stable, this correlation between the JT-elongated (and, hence, average) bond lengths and the stability of the JT isomers, with shorter bonds in the less stable JT configurations, implies a potential mechanism for the JT switching. Specifically, we propose that the pressure-induced distortion of the Cu coordination geometry progressively destabilizes one JT isomer relative to a less intrinsically stable, but undistorted JT configuration. Beyond a threshold pressure, the initial JT isomer becomes sufficiently distorted that an alternate less distorted, more compact JT isomer becomes more energetically favorable, at which point the JT-switching occurs.

Variable temperature magnetic susceptibility data were collected for pressure loadings up to 1.16 GPa (Figure 3). For phase I ( $P < 0.9$  GPa), the orientation of the magnetic orbital in the  $\text{CuF}_2\text{O}_2$  plane, in which the  $\text{Cu}^{\text{II}}$  centers are linked by a strong two-dimensional hydrogen-bonding lattice, provides for  $\text{Cu-OH}\cdots\text{F-Cu}$  spin-exchange paths. Broad maxima occur at 7–10 K with long-range antiferromagnetic ordering at 2.5 K. Following the JT-switch at pressures above 0.9 GPa, the re-orientation of the magnetic orbital to the  $\text{CuF}_2\text{N}_2$  plane permits only linear spin exchange paths along the Cu–pyz–Cu chains. The broad maximum at 3.7 K is indicative of one-dimensional antiferromagnetic coupling, with no indication of long range order above 2 K. As such, the JT-switch corresponds to an abrupt magnetic transition from two-dimensional to one-dimensional magnetic coupling. The spin lattice of phase III, with the magnetic orbital in the  $\text{CuO}_2\text{N}_2$  plane, should be analogous to phase II by maintaining the one-dimensional spin exchange paths along the Cu–pyz–Cu chains.

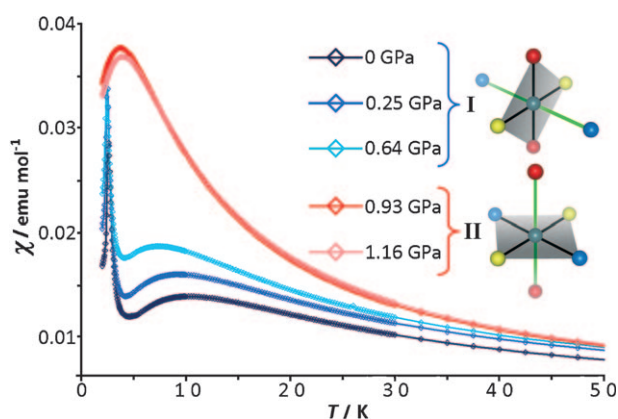


**Figure 3.** Variable-temperature magnetic susceptibility data for pressure loadings representative of phases I and II of  $\text{CuF}_2(\text{H}_2\text{O})_2(\text{pyz})$ .

In summary, the  $\text{CuF}_2\text{O}_2\text{N}_2$  octahedra of  $\text{CuF}_2(\text{H}_2\text{O})_2(\text{pyz})$  undergoes a successive switching of the JT axis from the N–Cu–N to the O–Cu–O to the F–Cu–F bonds reversibly as pressure is increased. This sequence occurs predictably in order of spectrochemical series, with the JT-axis switching from the pyz to the  $\text{OH}_2$  to the  $\text{F}^-$  ligand direction. Detailed structural analyses revealed that the likely mechanism underlying this unprecedented phenomenon involves the destabilization of successive JT-isomers through pressure-induced structural distortions of the  $\text{Cu}^{\text{II}}$  coordination environment to the point where a different JT isomer becomes favored. The accompanying switching of the magnetic orbital is reflected by an abrupt and reversible change in the magnetic properties from two-dimensional to one-dimensional coupling. This pressure-induced sequential JT-switching may be expected in a broad range of molecule-based magnetic materials, particularly those with asymmetric ligand coordination environments. More generally, this work demonstrates that pressure can be used to predictably control structure–property relationships in functional molecular materials, with broad implications for the development of next generation molecule-based magneto-electronic devices.

### Experimental Section

The pressure-dependent structure of  $\text{CuF}_2(\text{H}_2\text{O})_2(\text{pyz})$  was probed using synchrotron-based powder diffraction for the sample within a diamond anvil cell pressure apparatus. Crystals were prepared according to the previously published method.<sup>[5]</sup> In situ X-ray diffraction data ( $\lambda = 0.61832 \text{ \AA}$ ) were collected at the 1-BM beamline at the Advanced Photon Source, Argonne National Laboratory at 30 different pressures in the range 0–4.6 GPa. Polycrystalline  $\text{CaF}_2$  was included as an internal pressure marker, and isopropyl alcohol was used to mediate hydrostatic compression. Lattice parameters were determined from Le Bail fits to the diffraction data within GSAS.<sup>[11]</sup>

Additional structural parameters were refined using the Rietveld method.

Pressure-dependent magnetic susceptibility data were collected with a Quantum Design MPMS-7XL SQUID using a piston-based pressure cell (MCell 10, EasyLab Industries, with maximum pressure of 1.2 GPa). Polycrystalline  $\text{CuF}_2(\text{H}_2\text{O})_2(\text{pyz})$  was loaded in the cell with Daphne oil pressure transmitting fluid and a Sn pressure standard. Variable temperature data were collected for pressure loadings up to 1.16 GPa (Field: 400 G).

Received: June 3, 2010

Revised: July 9, 2010

Published online: September 10, 2010

**Keywords:** coordination frameworks · high-pressure chemistry · Jahn–Teller distortion · magnetic properties · X-ray diffraction

- [1] U.S. DOE, “Complex Systems: Science for the 21st Century” ([http://www.science.doe.gov/bes/reports/files/CS\\_rpt.pdf](http://www.science.doe.gov/bes/reports/files/CS_rpt.pdf)).
- [2] a) H. A. Jahn, E. Teller, *Proc. R. Soc. London Ser. A* **1937**, *161*, 220–235; b) L. R. Falvello, *J. Chem. Soc. Dalton Trans.* **1997**, 4463–4475.
- [3] a) K. W. Chapman, G. J. Halder, P. J. Chupas, *J. Am. Chem. Soc.* **2008**, *130*, 10524–10526; b) K. W. Chapman, P. J. Chupas, *J. Am. Chem. Soc.* **2007**, *129*, 10090–10091; c) M. Mito, T. Kawae, M. Takumi, K. Nagata, M. Tamura, M. Kinoshita, K. Takeda, *Phys. Rev. B* **1997**, *56*, R14255–R14258; d) I. R. Marsden, M. L. Alan, R. H. Friend, M. Kurmoo, D. Kanazawa, P. Day, G. Bravic, D. Chasseau, L. Ducasse, W. Hayes, *Phys. Rev. B* **1994**, *50*, 2118–2127; e) R. H. Friend, M. Miljak, D. Jerome, *Phys. Rev. Lett.* **1978**, *40*, 1048–1051.
- [4] Strictly speaking, the JT effect refers to the splitting of degenerate orbitals. Heteroligand systems, as present in  $\text{CuF}_2(\text{H}_2\text{O})_2(\text{pyz})$ , (with non-degenerate orbitals albeit orbitals of relatively similar energies), the corresponding effect is more accurately described as a pseudo-JT effect. However, while these are formally different from a theoretical perspective, the resulting structural distortions and underlying mechanisms are qualitatively comparable.<sup>[2b]</sup> As such, in the interest of clarity we have inclusively used “JT” as a general term for these effects.
- [5] J. L. Manson, M. M. Conner, J. A. Schlueter, A. C. McConnell, H. I. Southerland, I. Malfant, T. Lancaster, S. J. Blundell, M. L. Brooks, F. L. Pratt, J. Singleton, R. D. McDonald, C. Lee, M.-H. Whangbo, *Chem. Mater.* **2008**, *20*, 7408–7416.
- [6] C. Dobe, T. Strassle, F. Juranyi, P. L. W. Tregenna-Piggott, *Inorg. Chem.* **2006**, *45*, 5066–5072.
- [7] C. J. Simmons, M. A. Hitchman, H. Stratemeier, A. J. Schultz, *J. Am. Chem. Soc.* **1993**, *115*, 11304–11311.
- [8] S. Carlson, Y. Q. Xu, U. Halenius, R. Norrestam, *Inorg. Chem.* **1998**, *37*, 1486–1492.
- [9] D. F. Shriver, P. W. Atkins, *Inorganic Chemistry*, 5th ed., W. H. Freeman, **2010**.
- [10] K. W. Chapman, P. J. Chupas, *Chem. Mater.* **2009**, *21*, 425–431.
- [11] a) A. C. Larson, R. B. Von Dreele, Los Alamos National Laboratory Report, LAUR 86–748: **2000**; b) B. H. Toby, *J. Appl. Crystallogr.* **2001**, *34*, 210–213.